

# Silicon Anti-Phase Optical Coatings for High-Power, Single-Mode Operation in Vertical-Cavity Surface-Emitting Lasers

Kevin Pikul<sup>1</sup>, Leah Espenhahn, Patrick Su, Mark Kraman, John M. Dallesasse<sup>2</sup>

University of Illinois at Urbana-Champaign, Department of Electrical and Computer Engineering, Urbana, Illinois, 61801  
Tel: 1-(815)-582-9124, Email: kpikul2@illinois.edu<sup>1</sup>, jdalleasa@illinois.edu<sup>2</sup>

**Keywords:** Vertical-cavity surface-emitting lasers, high output power, single-transverse mode, silicon anti-phase coating

Single-layer silicon annular optical coatings are deposited atop oxide-confined vertical-cavity surface-emitting lasers (VCSELs) to enable preferential operation in a single-fundamental mode with enhanced optical output power. By disrupting the electric-field standing-wave pattern overlap with the active region, a spatially varying threshold modal gain can be achieved, suppressing the higher-order-transverse modes. This work examines the enhancements of the anti-phase coating on electro-optic performance and spectral characteristics of 850 nm AlGaAs-based VCSELs.

## INTRODUCTION

The growing commercial interest in optical depth sensing in 3D-facial recognition systems, LiDAR in autonomous vehicles, and eye tracking in AR/VR headsets has reinvigorated research and development into next-generation VCSEL technology. These applications challenge current VCSEL performance, requiring characteristics such as single-transverse-mode operation with high optical output powers. Historically, the first effective method of transverse mode control in VCSELs was selective  $\text{Al}_x\text{Ga}_{1-x}\text{As}$  oxidation [1,2] to confine optical and electrical carriers. However, the reduced active region diameter negatively affected output power. Therefore, the development of independent methods to control optical modes and confine current carriers was needed. The mode-control techniques from these efforts utilized methods that removed selective portions of the top Distributed Bragg Reflector (DBR) mirror, including surface-relief etching [3] and photonic crystals [4]. While these methods have resulted in single-mode operation, output power is reduced due to less efficient current injection caused by etching of the top p-type DBR mirror. Current cannot flow where material has been removed. This provides motivation for the focus of this work: satisfying the need for an additive mode-suppression technique using an optical coating that will enable higher powers while operating in a single-fundamental mode.

## ANTI-PHASE COATING DESIGN

Mode-suppression techniques are based on taking advantage of the spatial variation in energy across the open aperture inherent to VCSEL transverse modes. By selectively

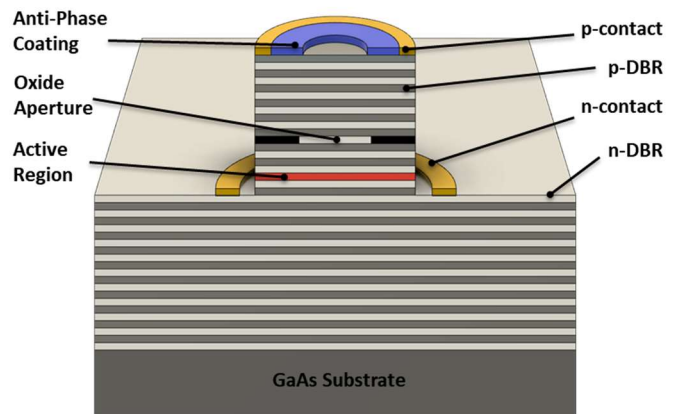


**Fig. 1** Anti-Phase-Coating VCSEL cross-sectional schematic diagram.

raising (or lowering) the threshold modal gain of a specific mode, its capability to lase will be suppressed (or enhanced). In previous multilayer dielectric optical coatings [5], several limitations with the VCSEL top DBR design, available coating materials, and need for a multi-step deposition and patterning process hindered the performance of the devices. Further efforts in redesigning the epitaxial material and coating have been performed here, yielding a simplified structure and coating as shown in Figure 1. With a complete mirror, the threshold modal gain for all modes is minimized. Therefore, in order to leave the fundamental mode unchanged while maximizing the threshold modal gain for the higher-order modes, a single  $\lambda/4$ -thick layer of silicon is deposited atop the p-type DBR and patterned in the shape of an annulus. The silicon/air interface creates out-of-phase (anti-phase) reflections back into the cavity that disrupt the standing wave pattern of the structure *only* in the regions where the silicon resides: the outer perimeter of the device, overlapping with the higher-order modes. The change in the standing wave pattern reduces the magnitude of the electric field overlapping the quantum well active region, thereby increasing the threshold modal gain and suppressing the capability of those modes to lase. Silicon is used due to its high refractive index compared to other dielectric materials (such as  $\text{TiO}_2$  and  $\text{SiO}_2$ ), which enhances the impact on modal gain. Additionally, it can be readily deposited in a standard cleanroom via electron-beam evaporation or magnetron sputtering. Because the optical thickness of the coating is

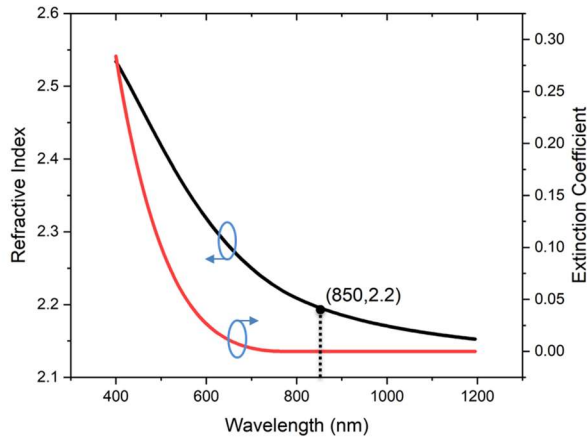


**Fig. 2** Optical constants of electron-beam evaporated silicon, with a value of 2.2 at the target wavelength of 850 nm.

crucial to obtaining ideal performance, the thickness and index of refraction must be carefully calibrated and monitored. However, in the event an undesirable coating is formed, the process is reversible and the coating thickness can easily be fine-tuned in a standard Reactive Ion Etching (RIE) system without damaging the GaAs cap layer. The irreversibility and lack of capability to fine-tune performance remains a drawback of both photonic crystals and surface relief due to their sensitivity to depth and destructive nature (removal of DBR layers).

#### DEVICE FABRICATION

The epitaxial material in this work was grown via MOCVD and designed for 850 nm operation. The devices follow a standard oxide-confined VCSEL process flow, beginning with a mesa etch in a chlorine-based Inductively Coupled Plasma (ICP)-RIE dry etching system followed by a wet oxidation process to form a 3  $\mu\text{m}$  oxidation aperture (OA). Next, AuGe/Ni/Au n-contacts are deposited and annealed to form ohmic contacts, followed by planarization with benzocyclobutene (BCB) to provide electrical insulation. A contact via is then etched using a fluorine-based RIE dry etching system. Afterwards, a Ti/Au interconnect layer and a Ti/Pt/Au p-contact are deposited and annealed. Before the final deposition onto the fabricated devices, the film's refractive index is characterized via spectroscopic ellipsometry. This process includes depositing the film onto a quartz witness sample in an electron-beam evaporator with a current of 60 mA and chamber pressure of  $\sim 1\text{E-}6$  Torr, resulting in a deposition rate of  $\sim 1$   $\text{\AA}/\text{s}$ . Afterwards, the sample is scanned and parameterized, and optical constants are generated as shown in Figure 2. Current films have a lower-than-expected refractive index value of 2.19 at 850 nm compared to literature values of 3.8 [6] for amorphous silicon. This is likely due to the e-beam current, which has

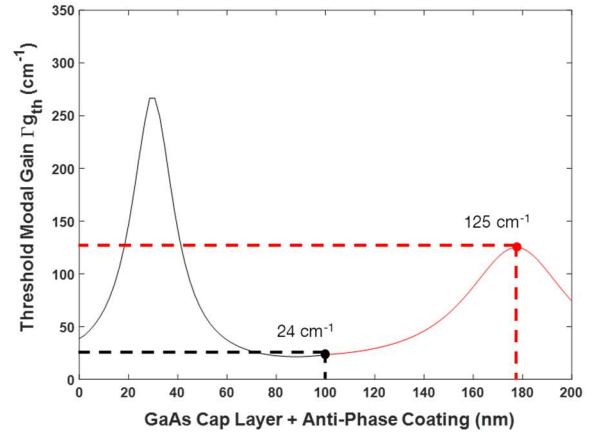


**Fig. 3** Threshold modal gain of VCSEL structure, indicating a null without the silicon coating, and a peak value of  $125\text{ cm}^{-1}$  at a coating thickness of 77 nm.

subsequently been increased to allow for less columnar growth and enhanced densification of the film [7]. Once the optical constants are measured, transfer matrix method (TMM) simulations are done to generate the electric-field standing wave pattern, followed by the threshold modal gain of the structure with the current silicon film. This is shown in Figure 3, where the threshold modal gain of the base structure is minimized at  $24\text{ cm}^{-1}$  with a GaAs cap layer 100 nm thick. With the presence of the silicon anti-phase coating, the threshold modal gain increases from  $24\text{ cm}^{-1}$  to  $125\text{ cm}^{-1}$  at a thickness of  $\sim 77$  nm. Upon completion of the film characterization, the coatings are deposited via e-beam evaporation and patterned onto the devices via a photolithographic liftoff process. Due to nonideal deposition conditions the film is purposely over deposited and etched down to the target thickness of 77 nm; thickness and coating anisotropy measurements are finally completed via Atomic Force Microscopy (AFM).

#### DEVICE CHARACTERIZATION

The devices were characterized for electro-optic performance via light-current-voltage (LIV) curves, and spectral characteristics via optical spectra measurements. Fig. 4 exhibits 3  $\mu\text{m}$  active region devices with 3 different coating structures: the baseline device with no coating, a non-patterned blanket coating, and patterned coatings. The small active region allows for inherent lasing in a single-fundamental mode (SMSR  $> 30$  dB) in the baseline device, with a maximum output power of 4.9 mW. Due to the anti-phase coating lowering the top DBR reflectivity, there is a significant increase in output power for the VCSELs with both patterned and non-patterned coatings. Interestingly, the lack of mode selectivity associated with the blanket coating disrupts single-mode operation even with this small oxide aperture size, with multiple higher-order modes lasing and

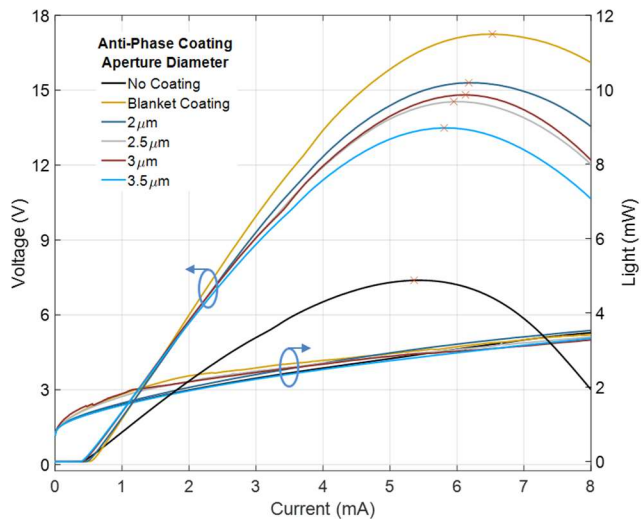


**Fig. 4** LIV family of curves for 3  $\mu\text{m}$  oxide aperture VCSELs with varying coating aperture sizes.

generating the most output power at 11.6 mW. The patterned devices behavior illustrates the potential for the anti-phase coating in fabricating high-power, single-mode VCSELs. The measured optical spectra of the device with a 2  $\mu\text{m}$  aperture in the coating is shown in Fig. 5, showing single-fundamental-mode operation through the entire current injection range up to thermal rollover at 6 mA. Moreover, a maximum single-mode output power of 10.2 mW is achieved, a 137% increase compared to the baseline device. As the aperture size increases, single-mode operation is maintained in the devices while the output power drops to a peak of 8.8 mW for the largest 3.5  $\mu\text{m}$  aperture device. The increase in output power results from the increased mirror loss in the top DBR, which is confirmed with the increase in threshold current.

## CONCLUSION

Anti-phase coatings have been shown to enhance VCSEL single-mode performance. These coatings present the potential for an easily manufacturable and tunable additive mode-control technique that achieves high-power single-mode operation. By further enhancing the deposition process, and therefore film quality, anti-phase coatings capable of suppressing higher-order modes in larger, inherently multimoded VCSELs is expected.

## ACKNOWLEDGEMENTS

This work is sponsored by the Coherent/II-VI Foundation under the Block-Gift program. This work was carried out in part in the Materials Research Laboratory Central Research Facilities at the University of Illinois Urbana-Champaign.

## REFERENCES

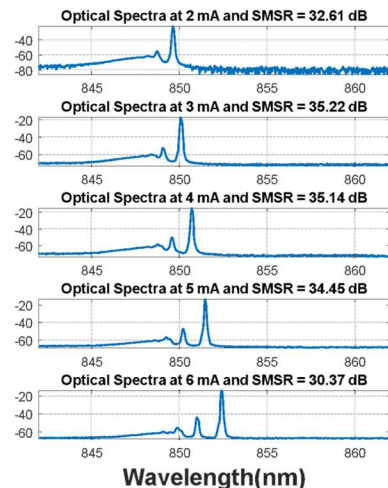


**Fig. 5** Measured optical spectra of VCSELs with a 2  $\mu\text{m}$  anti-phase coating aperture.

- [1] Dallesasse, John Michael, et al. "Hydrolyzation oxidation of  $\text{Al}_x\text{Ga}_{1-x}\text{As}/\text{AlAs}/\text{GaAs}$  quantum well heterostructures and superlattices." *Applied Physics Letters* 57.26 (1990): 2844-2846.
- [2] Huffaker, J. D., et al. "Native-oxide defined ring contact for low threshold vertical-cavity lasers." *Applied Physics Letters* 65.1 (1994): 97-99.
- [3] Unold, Heiko J., et al. "Large-area single-mode VCSELs and the self-aligned surface relief." *IEEE Journal of Selected Topics in Quantum Electronics* 7.2 (2001): 386-392.
- [4] Song, Dae-Sung, et al. "Single-fundamental-mode photonic-crystal vertical-cavity surface-emitting lasers." *Applied Physics Letters* 80.21 (2002): 3901-3903.
- [5] Kesler, Benjamin, et al. "Facilitating single-transverse-mode lasing in VCSELs via patterned dielectric anti-phase filters." *IEEE Photonics Technology Letters* 28.14 (2016): 1497-1500.
- [6] Pierce, Daniel T., and Wo E. Spicer. "Electronic structure of amorphous Si from photoemission and optical studies." *Physical Review B* 5.8 (1972): 3017.
- [7] Haque, S. Maidul, et al. "E-Beam Evaporation of Silicon: Native Oxidation and Quasicontinuous Tailoring of Optical Properties." *physica status solidi (a)* 218.22 (2021): 2100299.